Parameter Estimation from the Cross-Spectrogram Reassignment Vectors

Maria Sandsten
Centre for Mathematical Sciences
Lund University
Lund, Sweden
maria.sandsten@matstat.lu.se

Isabella Reinhold
Centre for Mathematical Sciences
Lund University
Lund, Sweden
isabella.reinhold@matstat.lu.se

Rachele Anderson
Centre for Mathematical Sciences
Lund University
Lund, Sweden
rachele.anderson@matstat.lu.se

***Abstract*—In this paper we propose a novel technique to estimate the parameters of two Gaussian envelope oscillatory signals, with the same time-locations and oscillatory frequencies but possibly different phases. The phase difference and the length of the Gaussian envelope are estimated directly from the slopes of the corresponding cross-spectrogram reassignment vectors. Including the phase difference and the envelope length in the scaled reassignment of the cross-spectrogram will give a perfectly concentrated time-frequency spectrum where the location of the maximum gives estimates of the time and oscillatory frequency parameters. The proposed method is evaluated for different SNRs and is also compared to state-of-the-art techniques for phase estimation of oscillatory electrical activity measured from the brain.**

***Index Terms*—time-frequency reassignment, oscillating transient signals, parameter estimation, phase estimation, EEG**

I. INTRODUCTION

The use of time-frequency (TF) methods has increased in many application areas, where signals often are multi-component and non-stationary, e.g. vibration analysis, radar detection, geophysics, and medicine. Most methods aim at increased concentration of components and suppression of cross-terms using the quadratic class of TF representations [1]. In recent years, most focus has been directed to instantaneous frequency estimation of linear and non-linear frequency modulated signals. In this area, numerous methods have been proposed with different treatment of the TF representation, e.g. eigenvector decomposition [2], image enhancement [3], and compressed sensing [4], [5]. The TF reassignment [6], and the related invertible synchrosqueezing [7], two well known techniques for sharpening the TF representation, have also been further developed e.g. [8]–[10].

For short oscillating transient signals we have recently invented novel techniques and corresponding underlying theory. We have shown that a Gaussian envelope oscillatory signal can achieve perfect time- and frequency localization, i.e. localization to one single time-frequency point, using a scaled reassignment technique, where the scaling is controlled by the combination of the spectrogram window and the Gaussian envelope [11], [12]. The method has been applied for characterization of transient components within the echolocation beam of a dolphin [13], [14]. We have further shown that a short transient of arbitrary envelope can achieve perfect time- and frequency localization with use of the matched window in a reassigned spectrogram [15]–[17] and explored the technique into a phase synchronization detection method [18].

In this paper we investigate the cross-spectrogram reassignment vectors and derive the formulas for estimating the set of parameters, which is modeling Gaussian envelope transient signal pairs. We start with a short presentation of the scaled reassigned spectrogram in section 2 followed by the derivation of the cross-spectrogram reassignment in section 3. In section 4, the performance of the proposed technique compared to state-of-the-art estimators is evaluated, especially for estimation of phase difference. An example of phase estimates from transient responses in the measured electrical activity from the brain is also given. Conclusions are presented in section 5.

II. THE SCALED REASSIGNED SPECTROGRAM

The reassigned spectrogram of the signal $x(t)$ is defined as

$$RS_x^h(t,\omega) = \iint S_x^h(s,\xi)\delta(t-\hat{t}_x(s,\xi),\omega-\hat{\omega}_x(s,\xi))dsd\xi, \quad (1)$$

where $\delta(t,\omega)$ is the two-dimensional Dirac impulse, integrals run from $-\infty$ to ∞ and $S_x^h(t,\omega) = |F_x^h(t,\omega)|^2$ with the short time Fourier transform (STFT)

$$F_x^h(t,\omega) = \int x(s)h^*(s-t)e^{-i\omega s}ds, \quad (2)$$

where * denotes complex conjugate. The reassignment vectors $\hat{t}_x$ and $\hat{\omega}_x$, are defined as

$$\hat{t}_x(t,\omega) = t + c_t\Re\left(\frac{F_x^{th}(t,\omega)}{F_x^h(t,\omega)}\right), \quad (3)$$

$$\hat{\omega}_x(t,\omega) = \omega - c_\omega\Im\left(\frac{F_x^{\frac{dh}{dt}}(t,\omega)}{F_x^h(t,\omega)}\right), \quad (4)$$

where $\Re$ and $\Im$ represents real and imaginary parts, $F_x^{th}(t,\omega)$ and $F_x^{\frac{dh}{dt}}(t,\omega)$ are the STFTs, with $t\cdot h(t)$ and $dh(t)/dt$ used as window functions.

We define a Gaussian windowed constant frequency signal

$$x(t) = g(t-t_0)e^{i\omega_0 t-\phi_0}, \quad (5)$$

This work was partially supported by the Wallenberg Autonomous Systems and Software Program (WASP) funded by Knut and Alice Wallenberg Foundation.

where t_0 is the time location, ω_0 the oscillating frequency, ϕ_0 the phase and

$$g(t) = e^{-\frac{t^2}{2\sigma^2}}, \quad -\infty < t < \infty, \tag{6}$$

is the transient envelope shape with scaling parameter σ. In [11] we have shown that a unit energy Gaussian window with scaling parameter λ,

$$h(t) = 1/(\pi^{1/4}\sqrt{\lambda})e^{-\frac{t^2}{2\lambda^2}}, \tag{7}$$

will result in the following reassignment vectors

$$\hat{t}_x(t,\omega) = t - c_t\left(\frac{\lambda^2}{\lambda^2+\sigma^2}\right)t, \tag{8}$$

$$\hat{\omega}_x(t,\omega) = \omega - c_\omega\left(\frac{\sigma^2}{\lambda^2+\sigma^2}\right)\omega. \tag{9}$$

The reassigned spectrogram according to Eq. (1) will be perfect time-frequency localized with all mass centered at time t_0 and frequency ω_0 for

$$c_t = \frac{\lambda^2+\sigma^2}{\lambda^2}, \quad c_\omega = \frac{\lambda^2+\sigma^2}{\sigma^2}. \tag{10}$$

In general σ is unknown, and one approach suggested in [12] estimates σ by evaluation of the resulting reassigned spectrogram concentrations for a number of candidate σ.

III. PHASE-CORRECTED REASSIGNED SPECTROGRAM

We now define pairs of oscillating transients with different amplitudes and phases as

$$y_n(t) = A_n g(t-t_0)e^{i\omega_0 t - \phi_n} \quad n = 1,2 \tag{11}$$

The complex-valued cross-spectrogram using the window $h(t)$ in Eq. (7) is

$$S^h_{y_{12}}(t,\omega) = F^h_{y_1}(t,\omega)(F^h_{y_2}(t,\omega))^*, \tag{12}$$

where

$$F^h_{y_n}(t,\omega) = A_n e^{-i\phi_n} F^h_x(t,\omega), \tag{13}$$

which relates to $x(t)$ as defined in Eq. (5). Example data is seen in Figure 1a of $y_1(t)$ and $y_2(t)$ with $t_0 = 100$, $\omega_0 = 2\pi 0.0625$, $A_1 = A_2 = 1$ and $\phi_2 - \phi_1 = \pi/4$. The Gaussian envelope parameter is $\sigma = 12$ and in Figure 1b the signals are depicted with a Gaussian white noise disturbance, SNR=10 dB, where SNR is defined as the average power of the signal within $\pm 3\sigma$ of the envelope to the noise variance. In Figure 1c the corresponding cross-spectrogram absolute value is depicted using a Gaussian window with $\lambda = 18$.

We study the case when $A_1 = A_2 = 1$ and use Eq. (13) with $h(t)$ replaced with $th(t)$ and $dh(t)/dt$ respectively. We use

$$F^{th}_x(t,\omega) = -\frac{\lambda^2}{\lambda^2+\sigma^2}\left(t + i\sigma^2\omega\right)F^h_x(t,\omega), \tag{14}$$

and the proportionality relation

$$F^{dh/dt}_x(t,\omega) = -(1/\lambda^2)F^{th}_x(t,\omega), \tag{15}$$

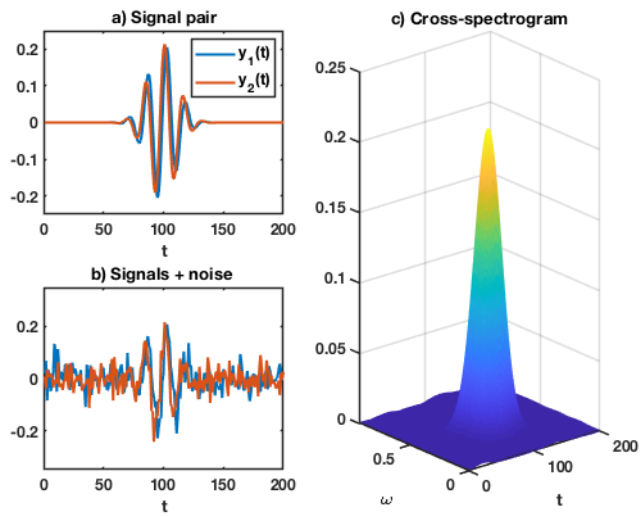

Fig. 1. a) The signal pair $y_1(t)$, $y_2(t)$ with $t_0 = 100$, $\omega_0 = 2\pi 0.0625$, $A_1 = A_2 = 1$ and $\phi_2 - \phi_1 = \pi/4$ and Gaussian envelope parameter $\sigma = 12$; b) Signals in white Gaussian noise disturbance, SNR=10 dB; c) The corresponding cross-spectrogram absolute value, for a window $h(t)$ with $\lambda = 18$.

derived in [11], giving the following expressions for the suggested cross-spectrogram reassignment vectors,

$$\frac{F^{th}_{y_1}}{F^h_{y_2}} + \frac{F^{th}_{y_2}}{F^h_{y_1}} = -\frac{\lambda^2(t+i\sigma^2\omega)}{\lambda^2+\sigma^2}(e^{i\Delta\phi} + e^{-i\Delta\phi}) \tag{16}$$

$$\frac{F^{\frac{dh}{dt}}_{y_1}}{F^h_{y_2}} + \frac{F^{\frac{dh}{dt}}_{y_2}}{F^h_{y_1}} = \frac{(t+i\sigma^2\omega)}{\lambda^2+\sigma^2}(e^{i\Delta\phi} + e^{-i\Delta\phi}) \tag{17}$$

where $\Delta\phi = \phi_2 - \phi_1$ and where t and ω on the left side of the equality are dropped for convenience. Following the general formulation of the reassignment vectors in Eqs. (3,4) we find that the real and imaginary parts of Eqs. (16,17) simplify into

$$CR(t,\omega) = \Re\left(\frac{F^{th}_{y_1}}{F^h_{y_2}} + \frac{F^{th}_{y_2}}{F^h_{y_1}}\right) = \frac{-2\lambda^2}{\lambda^2+\sigma^2}\cos(\Delta\phi)t \tag{18}$$

$$CI(t,\omega) = \Im\left(\frac{F^{\frac{dh}{dt}}_{y_1}}{F^h_{y_2}} + \frac{F^{\frac{dh}{dt}}_{y_2}}{F^h_{y_1}}\right) = \frac{2\sigma^2}{\lambda^2+\sigma^2}\cos(\Delta\phi)\omega, \tag{19}$$

where we note that $CR(t,\omega)$ is independent of ω and $CI(t,\omega)$ of t. We use the information from the above equations to find an estimate of $\cos(\Delta\phi)$ without actual knowledge of the component length parameter σ and we define the linear direction coefficient in t of Eq. (18) as

$$k_t = -\frac{2\lambda^2}{\lambda^2+\sigma^2}\cos(\Delta\phi), \tag{20}$$

the linear direction coefficient in ω of Eq. (19) as

$$k_\omega = \frac{2\sigma^2}{\lambda^2+\sigma^2}\cos(\Delta\phi). \tag{21}$$

From Eqs. (20,21) follows

$$-\frac{k_t - k_\omega}{2} = \cos(\Delta\phi). \tag{22}$$

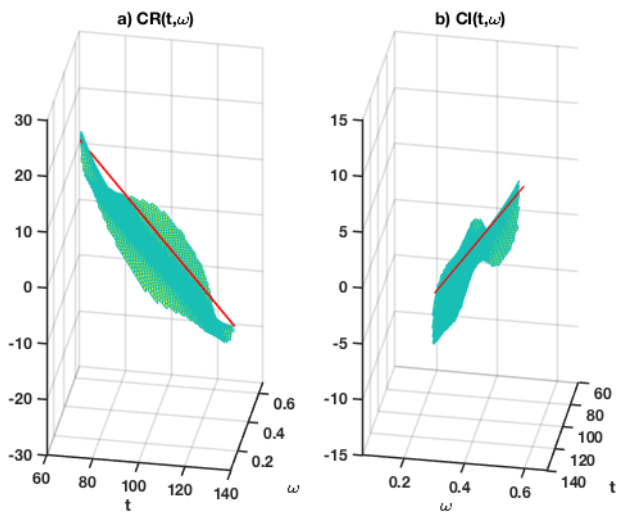

Fig. 2. a) $CR(t,\omega)$ and the estimated slope $\hat{k}_t \cdot t$, (red line) and b) $CI(t,\omega)$ and the estimated slope $\hat{k}_\omega \cdot \omega$, (red line), for the signal pair shown in Figure 1.

Estimates of k_t and k_ω are derived from the slopes of $CR(t,\omega)$ and $CI(t,\omega)$ in the directions t and ω respectively, close to t_0 and ω_0. We use all time- and frequency values where

$$|S^h_{y_{12}}(t,\omega)| > \max(|S^h_{y_{12}}(t,\omega)|) \cdot \epsilon, \quad 0 < \epsilon < 1, \tag{23}$$

and the slopes in respective direction t and ω are derived as the averages of the values in the perpendicular directions in the time-frequency range defined by Eq. (23) i.e. we extract the direction coefficients $\hat{k}_t$ and $\hat{k}_\omega$ from

$$\frac{1}{\omega_1(t)-\omega_0(t)} \int_{\omega_0(t)}^{\omega_1(t)} CR(t,\omega) d\omega = \hat{k}_t \cdot t, \tag{24}$$

$$\frac{1}{t_1(\omega)-t_0(\omega)} \int_{t_0(\omega)}^{t_1(\omega)} CI(t,\omega) dt = \hat{k}_\omega \cdot \omega. \tag{25}$$

In Figure 2, we show an example from the signal pair in Figure 1, where $CR(t,\omega)$ and $CI(t,\omega)$ are limited using $e = 0.2$ in Eq. (23) and the estimated slopes $\hat{k}_t \cdot t$ and $\hat{k}_\omega \cdot \omega$ are depicted with red lines. We also find

$$SR(t,\omega) = \Im\left(\frac{F^{th}_{y_1}}{F^h_{y_2}} - \frac{F^{th}_{y_2}}{F^h_{y_1}}\right) = \frac{-2\lambda^2}{\lambda^2+\sigma^2}\sin(\Delta\phi)t \tag{26}$$

$$SI(t,\omega) = \Re\left(\frac{F^{\frac{dh}{dt}}_{y_1}}{F^h_{y_2}} - \frac{F^{\frac{dh}{dt}}_{y_2}}{F^h_{y_1}}\right) = \frac{-2\sigma^2}{\lambda^2+\sigma^2}\sin(\Delta\phi)\omega. \tag{27}$$

The linear direction coefficients in t and ω of Eqs. (26,27) are

$$q_t = -\frac{2\lambda^2}{\lambda^2+\sigma^2}\sin(\Delta\phi), \quad q_\omega = -\frac{2\sigma^2}{\lambda^2+\sigma^2}\sin(\Delta\phi), \tag{28}$$

and

$$-\frac{q_t+q_\omega}{2} = \sin(\Delta\phi). \tag{29}$$

Estimates of q_t and q_ω are found in a similar way as for $\hat{k}_t$ and $\hat{k}_\omega$ and the final phase estimate is found as

$$\Delta\hat{\phi} = \text{atan}\left(\frac{-(\hat{q}_t+\hat{q}_\omega)}{-(\hat{k}_t-\hat{k}_\omega)}\right). \tag{30}$$

To perform a scaled reassigned spectrogram from the reassignment vectors in Eq. (10) we also need the component length parameter σ. We rely on the following formulation

$$\hat{\sigma} = \lambda\sqrt{\frac{1}{2}\left(\frac{\hat{q}_\omega}{\hat{q}_t} - \frac{\hat{k}_\omega}{\hat{k}_t}\right)}, \tag{31}$$

derived from Eqs. (20,21,28), where the window parameter λ is known. The scaled reassignment parameters c_t and c_ω can now be calculated as defined in Eq. (10) with an estimate of σ. To derive a reassigned cross-spectrogram we also correct for the phase-difference $\Delta\phi$ in the reassignment vectors according to

$$\hat{t}_{y_{12}}(t,\omega) = t + c_t\Re\left(e^{i\Delta\phi}\frac{F^{th}_{y_1}(t,\omega)}{F^h_{y_2}(t,\omega)}\right), \tag{32}$$

$$\hat{\omega}_{y_{12}}(t,\omega) = \omega - c_\omega\Im\left(e^{i\Delta\phi}\frac{F^{\frac{dh}{dt}}_{y_1}(t,\omega)}{F^h_{y_2}(t,\omega)}\right), \tag{33}$$

resulting in the phase-corrected reassigned spectrogram (PCRS),

$$PS^h_{y_{12}}(t,\omega) = \iint |S^h_{y_{12}}(s,\xi)|\delta(t-\hat{t}_{y_{12}}(s,\xi),\omega-\hat{\omega}_{y_{12}}(s,\xi))dsd\xi. \tag{34}$$

The parameters t_0 and ω_0 can be estimated from the time- and frequency locations of the peak. We also note that with use of the estimated σ, the usual scaled reassigned spectrograms from each signal $y_1(t)$ and $y_2(t)$ can be computed from Eq. (1) with the scaled reassignment parameters from Eq. (10).

IV. EVALUATION

A. Evaluation for different window lengths

We simulate real-valued transient oscillating signals $y_1(t)$ and $y_2(t)$, $t = 0\ldots199$, with Gaussian envelope shapes, $\sigma = 12$, as presented in Figure 1a. All signals have $t_0 = 100$ and $\omega_0 = 2\pi 0.0625$, $A_1 = A_2 = 1$, $\phi_1 \in U[0,2\pi]$ and $\phi_2 = \phi_1 + \Delta\phi$ where $\Delta\phi \in U[\pi/8, 3\pi/8]$ to avoid possible outlier estimates close to zero and $\pi/2$. Gaussian white noise is added to the signal, with SNR defined as the average power of the signal within $\pm 3\sigma$ of the envelope to the noise variance. All simulations are run with FFT-length 1024, which results in about the same number of bins in time- and frequency for a matched window spectrogram, $\lambda = 12$. For all SNRs the parameter ϵ in Eq. (23) is set to 0.2. We evaluate the performance of the proposed technique to estimate $\Delta\phi$, σ and thereafter t_0, ω_0 from the peak of the final PCRS. Four different window lengths are tested, $\lambda = 6$, 12, 18 and 24.

In Figure 3a, the resulting mean bias values of the estimated phase difference $\Delta\phi$ is depicted for different SNRs and the four window lengths. The bias is in all cases extremely small.

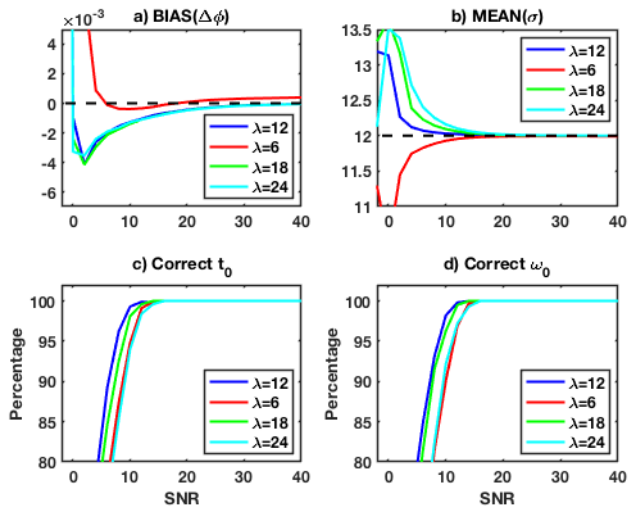

Fig. 3. a) Mean bias value of the estimated phase differences for different SNRs and four window lengths; b) Mean value for the estimated component length, (true value-dashed black line); c) Percentage of correct time estimates; d) Percentage of correct frequency estimates.

However, a thorough look will show that the shortest window continues to give a small bias also for high SNR. This can be explained by the fact the frequency is low and for shorter window lengths, the resulting spectrogram component width in frequency will be larger, with increasing effect of leakage from the negative frequency component. The standard deviations (stds) of the results from the different windows are more or less equal, and are not depicted. For SNR=10 dB we find the estimated studs close to 0.077 and the stds are exponentially decreasing for higher SNR.

In Figure 3b, the resulting mean values of the estimated component length are shown, where the true value, $\sigma = 12$, is marked as a dashed black line. We see that the best estimate is given by the matched window, $\lambda = 12$, followed by the longer window $\lambda = 18$ and then the shorter window $\lambda = 6$. The result indicates that the length of the window should be made equal or larger than the actual component length. This is intuitively explained by that a better estimate probably is received if the whole length of the component is included into the window in comparison to cutting the tails. However, with a too long window, the amount of noise becomes larger. The stds are not shown but are all comparable for the four different windows. For SNR=10 dB we find std values close to 0.715 and the stds are exponentially decreasing for increasing SNR.

Figure 3c and d show the final estimates of t_0 and ω_0, given from the location of the PCRS maximum peak. The resulting percentage of values with smaller error deviation than 3 samples are shown. The cross-spectrogram is calculated with λ and the scaled reassignment is based on the estimated $\Delta\hat{\phi}$ and $\hat{\sigma}$ in Figure 3a and b from the corresponding λ. The results are similar to the previous where the matched window $\lambda = 12$ has the best performance followed by the larger window $\lambda = 18$.

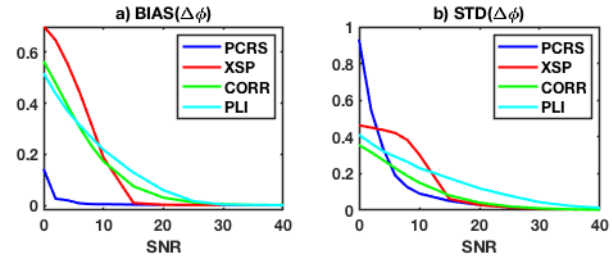

Fig. 4. a) and b) The average bias and standard deviation of the estimated phase differences for different SNRs and methods.

B. Phase-estimation compared to state-of-the-art methods

We use the same signal pair simulation as above with $\sigma = 12$. The disturbing white noise is exchanged to colored noise, similar to Electroencephalogram (EEG), generated from a simulation model as described in [19], with the noise balance parameters $\alpha = 4$, $\beta = 12$ and $\gamma = 0.5$ for the α, one-over-f and measurement noise activities respectively. The noise realizations are uncorrelated between channels and the SNR is defined as above, where the colored noise variance is calculated over the complete frequency range. The window parameter is $\lambda = 18$.

Estimates of $\Delta\phi$ from PCRS are compared with the results from state-of-the-art phase estimators, such as the commonly used time-based Pearson's linear correlation (CORR), time-frequency cross-spectrogram phase (XSP) [1], and Phase Lag Index (PLI) [20]. The cross-spectrogram of the XSP is computed using the window with $\lambda = 18$, and the phase values are extracted and averaged for all cross-spectrogram values where the absolute value exceeds 5% of the peak value. The PLI is calculated from the signals Hilbert transforms and the corresponding angle differences, reconstructed into positive or negative values using the sign operator, which is then finally averaged. Both the CORR and the PLI are limited to time values between 70-130 for all SNR as this time range gave the best performance.

The results of the PCRS show that the method is unbiased for SNRs down to 5 dB, where all other methods have large biases, see Figure 4a. The std of the PCRS is also lower than any other method down to 5 dB.

C. Real data example

We finally illustrate with an example of EEG data measured during visual stimulation with a 9 Hz flickering light (Grass Photic stimulator Model PS22C). Data was recorded using a Neuroscan system with a digital amplifier (SYNAMP 5080, Neuro Scan, Inc.). Amplifier band-pass settings were 0.3 and 50 Hz and sample rate was 256 Hz and later down-sampled to 128 Hz. The subject was supine with closed eyes and the light was flashed from a distance of approximately 1 m.

The light stimulation lasted just for the short time interval of about 1 s so the PCRS and XSP are based on a Gaussian window of 1.22 s to fulfill that better estimates are achieved when the window is longer than the transient. For the analysis

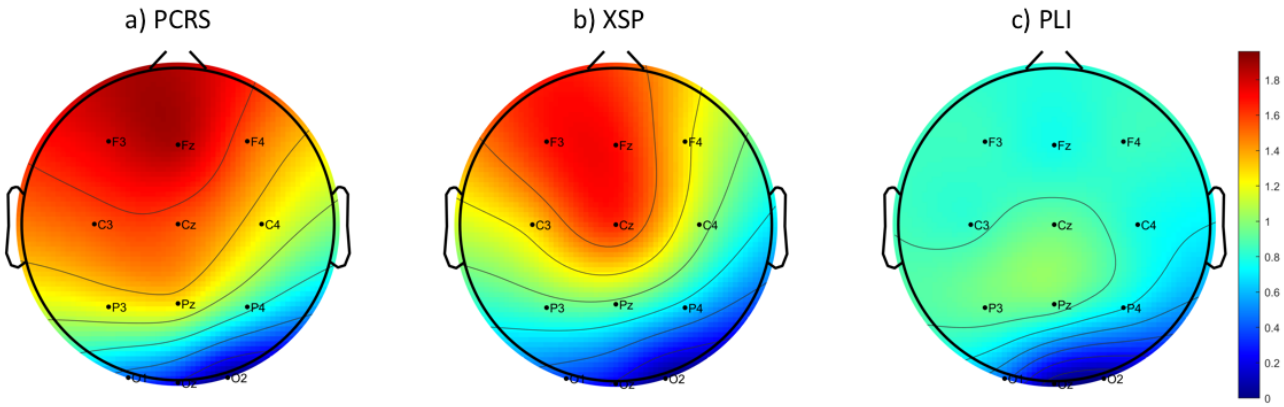

Fig. 5. The figure shows the estimated phase differences $\Delta\phi$ of all channels compared to channel O2 (located in the back to the right).

with CORR and PLI, the data was band-pass filtered limited to 7 and 15 Hz and further the time sampled used was 1 s of the detected response. Similarly, for the PCRS and XSP, the peak value of the cross-spectrogram was detected in the range 7 to 15 Hz and the 1 s range of the detected response. We show the results of the PCRS, XSP and PLI, but ignore CORR as the performance was not satisfactory. All channels are compared to the occipital channel O2, placed above the primary visual area to the right. We see the estimated phase patterns in Figure 5, with estimated $\Delta\phi$ presented in colours from zero to $2\pi/3$, where $2\pi/3$ corresponds to about 37 ms difference for a 9 Hz oscillations. The largest estimated phase differences are given from the PCRS and as expected from the frontal electrodes at the left side (F3 and Fz).

V. CONCLUSIONS

A technique for parameter estimation of pairs of Gaussian envelope oscillatory signals is proposed, where the cross-spectrogram reassignment vectors are directly used. The method is shown to outperform state-of-the-art methods for phase difference estimation in simulations of electrical brain activity. The estimated envelope parameter can further be used in the scaled reassigned spectrogram.

REFERENCES

[1] L. Cohen, *Time-Frequency Analysis*, ser. Signal Processing Series. Upper Saddle River, NJ, USA: Prentice-Hall, 1995.

[2] L. Stanković, D. Mandić, M. Daković, and M. Brajović, "Time-frequency decomposition of multivariate multicomponent signals," *Signal Processing*, vol. 142, no. 12, pp. 468–479, 2018.

[3] N. A. Khan and M. Sandsten, "Time-frequency image enhancement based on interference suppression in Wigner-Ville distribution," *Signal Processing*, vol. 127, pp. 80–85, 2016.

[4] J. Swärd, J. Brynolfsson, A. Jakobsson, and M. Hansson-Sandsten, "Sparse semi-parametric estimation of harmonic chirp signals," *IEEE Trans. on Signal Processing*, vol. 64, no. 7, pp. 1798–1807, 2016.

[5] E. Sejdić, I. Orović, and S. Stanković, "Compressive sensing meets time-frequency: An overview of recent advances in time-frequency processing of sparse signals," *Digital Signal Processing*, vol. 77, pp. 22–35, 2018.

[6] F. Auger and P. Flandrin, "Improving the readability of time-frequency and time-scale representations by the reassignment method," *IEEE Trans. on Signal Processing*, vol. 43, pp. 1068–1089, May 1995.

[7] I. Daubechies, Y. G. Wang, and H.-T. Wu, "ConceFT: concentration of frequency and time via a multitapered synchrosqueezed transform." *Phil. Trans. R. Soc. A*, vol. 374, no. 20150193, 2016.

[8] S. Meignen and P. Duong-Hung, "Retrieval of the modes of multicomponent signals from downsampled short-time Fourier transform." *IEEE Trans. on Signal Processing*, vol. 66, no. 23, pp. 6204 – 6215, 2018.

[9] K. Czarnecki, D. Fourer, F. Auger, and M. Rojewski, "A fast time-frequency multi-window analysis using a tuning directional kernel." *Signal Processing*, vol. 147, pp. 110 – 119, 2018.

[10] D. Fourer, F. Auger, and G. Peeters, "Local AM/FM parameters estimation: Application to sinusoidal modeling and blind audio source separation," *IEEE Signal Processing Letters*, vol. 25, no. 10, pp. 1600–1604, 2018.

[11] M. Hansson-Sandsten and J. Brynolfsson, "The scaled reassigned spectrogram with perfect localization for estimation of Gaussian functions," *IEEE Signal Processing Letters*, vol. 22, no. 1, pp. 100–104, 2015.

[12] J. Brynolfsson and M. Sandsten, "Parameter estimation of oscillating Gaussian functions using the scaled reassigned spectrogram," *Signal Processing*, vol. 150, pp. 20–32, 2018.

[13] I. Reinhold, M. Sandsten, and J. Starkhammar, "Objective detection and time-frequency localization of components within transient signals," *J. Acoust. Soc. Am. (JASA)*, vol. 143, no. 4, pp. 2368–2378, 2018.

[14] J. Starkhammar, I. Reinhold, P. W. Moore, D. S. Houser, and M. Sandsten, "Detailed analysis of two detected overlaying transient components within the echolocation beam of a bottlenose dolphin (tursiops truncatus)," *J. Acoust. Soc. Am. (JASA)*, vol. 145, no. 4, pp. 2138–2148, 2019.

[15] M. Sandsten, J. Brynolfsson, and I. Reinhold, "The matched window reassignment," in *EUSIPCO*, Rome, Italy, 2018.

[16] J. Brynolfsson, I. Reinhold, J. Starkhammar, and M. Sandsten, "The matched reassignment applied to echolocation data," in *Proceedings of the ICASSP*. Brighton, U.K.: IEEE, 2019.

[17] J. Brynolfsson, I. Reinhold, and M. Sandsten, "A time-frequency-shift invariant parameter estimator for oscillating transient functions using the matched window reassignment," *Signal Processing*, vol. 183, 2021.

[18] M. Sandsten, R. Anderson, I. Reinhold, and J. Brynolfsson, "The matched reassigned cross-spectrogram for phase estimation," in *Proceedings of the ICASSP*. Barcelona, Spain: IEEE, 2020.

[19] E. Barzegaran, S. Bosse, P. J. Kohler, and A. M. Norcia, "EEG-SourceSim: A framework for realistic simulation of EEG scalp data using MRI-based forward models and biologically plausible signals and noise." *Journal of Neuroscience Methods*, vol. 328, 2019.

[20] C. J. Stam, G. Nolte, and A. Daffertshofer, "Phase lag index: Assessment of functional connectivity from multi channel EEG and MEG with diminished bias from common sources." *Human Brain Mapping*, vol. 28, no. 11, pp. 1178–1193, 2007.